

A Lightweight U-Net Model for Accurate Skin Lesion Segmentation

Fallah H. Najjar

Karrar A. Kadhim

Farhan Mohamed

Mohd Shafry Mohd Rahim

Asniyani Nur Haidar Abdullah

Follow this and additional works at: <https://ijcsm.researchcommons.org/ijcsm>



Part of the [Computer Engineering Commons](#)



ORIGINAL STUDY

A Lightweight U-Net Model for Accurate Skin Lesion Segmentation

Fallah H. Najjar^{id a,b}, Karrar A. Kadhim^{id a,c}, Farhan Mohamed^{id a,*},
Mohd Shafry Mohd Rahim^{id a}, Asniyani Nur Haidar Abdullah^{id a,d}

^a Department of Emergent Computing, Faculty of Computing, Universiti Teknologi Malaysia, Johor Bahru, Malaysia

^b Department of Computer Systems Techniques, Technical Institute of Najaf, Al-Furat Al-Awsat Technical University, Najaf, 54001, Iraq

^c Computer Techniques Engineering Department, Faculty of Information Technology, Imam Ja'afar Al-Sadiq University, Baghdad, Iraq

^d Faculty of Information & Communication Technology, Universiti Teknikal Malaysia Melaka Hang Tuah Jaya, 76100 Durian Tunggal, Melaka, Malaysia

ABSTRACT

In this paper, a new lightweight U-Net deep learning-based neural network designed for the segmentation of skin lesions is proposed. Segmentation of skin lesions is the most critical step in computer-aided dermatology diagnosis for the early detection of melanoma and other diseases. However, we address the difficulty related to the precise definition of the lesion margins with an eye on the computation cost. We have demonstrated the state-of-the-art performance of DeepSkinSeg in most metrics on dermoscopic images using the PH2 and Human Against Machine (HAM10000) datasets. The metrics of the DeepSkinSeg model were robustness measured as the Intersection over Union (IoU) at 91.49, Dice coefficient at 95.56, precision at 97.97, sensitivity at 96.84, and accuracy at 96.71 for the PH2 dataset. Other standard generalization capabilities for the HAM10000 dataset could be an IoU of 92.97, a Dice coefficient of 96.36, precision at 97.64, sensitivity at 95.10, and an accuracy of 94.59. DeepSkinSeg has a very efficient inference because the model itself is lightweight, proving to be very helpful for real-time dermatological analysis. This work further advanced the computer-aided diagnosis in the task of skin lesion classification, guaranteeing even more promising clinical applications.

Keywords: Skin cancer, Skin lesion segmentation, DeepSkinSeg, PH2, HAM10000

1. Introduction

Most of the diseases affect people of all age groups, including infectious and non-infectious, chronic, or acute diseases [1]. Cancers belong to non-infectious conditions that prevail in human bodies because of uncontrolled cell division [2]. Cancer can occur in any organ of the body or at any stage of life, and in general, it takes the name of the organ or part from which it emanates. Of course, the most common types are breast, lung, prostate, skin, and intestine cancer. These factors include genetics, environmental exposures, and unhealthy practices such as smoking and making poor dietary choices. Lifestyle changes include quitting smoking, adopting a healthy diet, and

limiting exposure to the sun, all ways through which an individual might reduce his chance of getting some types of cancer [3]. Treatment modalities often used for cancer may include surgery, chemotherapy, radiation therapy, or a combination of several of the approaches described, all tailored to the cancer type and its stage, as well as general health [4, 5]. Skin cancer is one of the most common human malignancies, usually diagnosed by physical examination [6]. Skin diagnostic imaging techniques include ultrasonography, dermatoscopy, and reflectance confocal microscopy. Though these modalities have recently undergone improved changes and development [7], Skin cancer basically includes three main types: melanoma, squamous cell cancer, and basal cell

Received 18 September 2024; revised 30 November 2024; accepted 31 December 2024.
Available online 12 April 2025

* Corresponding author.
E-mail address: farhan@utm.my (F. Mohamed).

<https://doi.org/10.52866/2788-7421.1230>

2788-7421/© 2025 The Author(s). This is an open-access article under the CC BY license (<https://creativecommons.org/licenses/by/4.0/>).

cancer. The primary differentiation of the non-benign from the benign category is made through the texture and color of lesions combined with the cellular features [8]. Thus, the use of only visual imaging of skin cancer to identify it could be tricky with the type of variation that exists with the various types of skin cancer tumors [9]. In addition to its diagnostic complexity, different kinds of cues, such as patient information or whole imaging results, are necessary for reaching a proper diagnosis. Besides, medical images have had a much-welcoming influence in the field of medicine regarding diagnosis and planning treatment. The crux of medical images lies in the analysis to meet specified objectives. For example, the processing of skin cancer images has been found to be instrumental in regard to the process of image segmentation and has direct effects on the results of fusion [10]. In the context of planning treatment for skin cancer, accurate segmentation in medical images plays a pivotal role in the contouring process [2]. Automated image segmentation automatically facilitates the process of extracting object boundary features in an image [11]. Therefore, there is a need to be aware of image content for the very purpose of searching medical images. Therefore, medical image segmentation poses a complex and challenging problem marked by boundary deficiencies and a lack of texture contrast between regions of interest and the background [1, 3, 12]. However, its significant contributions can be listed as follows: i. to designing a new lightweight UNet model, DeepSkinSeg, for skin lesion segmentation. It simplifies the original UNet architecture while maintaining the strength of efficiency by reducing the number of layers without affecting the accuracy of skin lesion segmentation. ii. The performance of DeepSkinSeg shall be evaluated with a wide range of experiments conducted over popular databases like PH2 and HAM10000. iii. Numerical results on the PH2 and HAM10000 datasets show that the DeepSkinSeg gives a notable improvement over existing state-of-the-art methods in terms of the IoU, Dice coefficient, precision, recall, and accuracy metrics.

2. Related works

This section describes the theory needed to understand recent work on skin cancer segmentation in the literature. Tang et al. [13] used a separable-Unet model with the addition of stochastic weight averaging and proposed a model to segment skin lesions. Herein, we exploit the U-Net structure and point-wise separable convolution to effectively capture the context features' correlations and high-level semantic information with discriminative power advanced

from pixel to pixel for fully convolutional networks (FCNs), which helps in a great way to alleviate the problem of overfitting in essence, being trapped within local or suboptimal solutions via stochastic weight averaging. This technique helps gain a more enlarged optimum, which further aids in better model generalization. Nevertheless, the approach of the authors is local, and the only limitation is related to the operation of filling binary holes to enhance the segmentation results.

Qiu et al. [14] introduced a skin lesion segmentation technique using an ensemble of deep models: the convolutional neural network (DCNN) with fully connected conditional random fields (CRFs). Ensemble learning, on the other hand, with more than one DCNN model ensemble in combination with the CRF inference, handles the probabilistic inferences using random fields across dermoscopy images. The main disadvantage of their approach is that it is conditioned by the quality of the lesion segmentation given by the DCNN models. If the initial segmentations given by the DCNN models are of a low-quality profile, the general performance of this method may be degraded.

Tang et al. [15] proposed a Multi-Scale Context-Guided Network (MSCGnet) for accurate skin lesion segmentation, which aggregates multi-scale context information to improve feature encoding. Thus, with the information lost by spatial downsampling, we propose a context-aware attention structure (CAs) to rediscover and employ the important context features at the decoding end. Thus, they build an iterative version, iMSCGnet, by going through many iterations in order to make this version refine its accuracy. The authors trained iMSCGnet using a new deep supervision objective function, which encourages end-to-end training and integrates contributions from encoding layers and outputs of each iteration of iMSCGnet. However, iMSCGnet can only evaluate the processing of the low-level context information, hence its drawback. The other challenge in this regard is that ambiguous lesions are sometimes tricky to localize accurately within the area.

Dayananda et al. [16] also introduced an encoder-decoder structured lesion segmentation strategy in the skin. They build their method using Spatial Group Convolutions (SGC) for the first time in an encoder-decoder structure. They used 1×1 , 3×3 , 5×5 , and 7×7 . A series of $k \times 1$, $1 \times k$ convolutions go through each $k \times k$ kernel operation. This use of large kernels through two 1-D convolutions builds up the receptive field of the model so that it is able to increase the potential to pull features, yet at the same time, does not have an over-increase in the number of parameters it has to learn. The use of several kernel sizes helps capture all the discriminative features used. However,

their performance outcomes in terms of segmentation accuracy were actually not high.

Hu et al. [17] proposed a novel and robust Attention Synergy Network (AS-Net) for enhanced discrimination ability for skin lesion segmentation by the combination of spatial and channel attention mechanisms. It will identify lesion-specific features by tapping the abilities of the channel attention mechanism to focus attention on that specific dimension and, at the same time, exploit the synergy of these spatial and channel insights. They also introduced an enhanced weighted binary cross-entropy loss function to enhance the foreground lesion attention. The inclusion of the pre-trained VGG model does help in performing better for the given task but adds up the computation and time required to train the model.

Deepa and Madhavan [18] presented an advanced deep-learning model to enhance the process of segmenting skin lesions in medical images. The methodology involves two main phases: pre-processing images and applying the Adaptive Boundary-aware Transformer with a Gated Attention Mechanism (ABT-GAMNet). However, one limitation is the challenging nature of lesion image segmentation due to significant similarities in lesion morphology, such as occluding hair, structure size, shape, and intrinsic image attributes like contrast and skin pigmentation.

A transformer-based, multi-attention hybrid network called TMAHU-Net is presented by Dong et al. [19] and designed for learning the delicate and intricate patterns within skin lesion areas. It features an innovative hybrid module that perfectly combines the advantages of CNN (Convolutional Neural Networks) and transformer technology, making it possible to bring both wide-ranging global detail and localized feature information. The network is comprised of deep separable convolutional attention mechanisms that adaptively set the attention weight smartly and greatly enhance the quality of the learned representation of features in both channel and space dimensions. On the other hand, TMAHU-Net is designed to cater to skin lesion segmentation, yet it suffers from localization difficulty for exact detection in positive instances within some selected datasets.

Li et al. [20] put forward a new approach, the Uncertainty Self-Learning Network (USL-Net), to delve into the existing gap in handling segmentation tasks without reliance on the ground truth of labels. It first applies contrastive learning in feature extraction, which helps guide the creation of Class Activation Maps (CAMs) to serve as saliency maps. Regions of high saliency within these maps are picked and used as pseudo-labels of the regions matching the lesion, while areas of low saliency are considered to belong to the background. In this example, intermediate re-

gions would be those that are hard to classify, usually located on the border of lesions, or have artifacts such as hair or blisters. These are excluded from pseudo-labeling so that they are not confused by mistakes and confusion from learning about the network itself. The authors also proposed connectivity and centrality detection techniques to ensure the truthfulness of the foreground pseudo-labels further and, hence, reduce errors due to noise. While these advances have gone a long way toward improving the performance of unsupervised segmentation, USL-Net fails to reach the performance level that many of the supervised methods achieve. These challenges and limitations are further evidently present in regions with purple iodophor or hair artifacts, and it is hard for USL-Net to capture these features for pseudo-labeling.

Srikanteswara and Ramachandra [21] proposed an approach to the early detection of skin melanoma using the Adaptive Contour Model (ACM), in which they took into consideration noise in an image, obtaining quality segmentation and considering most of the contour features. However, the method also has a scope in the results within which it is circumscribed.

3. Methodology

The methodology for our proposed DeepSkinSeg network follows a structured approach to skin lesion segmentation, employing an encoder-decoder architecture widely recognized for its efficacy in medical image processing. The detailed methodology is as follows: The encoder section of DeepSkinSeg is designed to progressively condense the spatial dimensions while enhancing the depth of the input image features. It includes a collection of convolutional layers with batch normalization and ReLU functions in each of its blocks. In order to capture the different types of intricate spatial features within the image, the convolutional layers are applied with different filters. Subsequent batch normalization ensures the output normalizes, thereby mitigating the internal covariate shifts and, therefore, stabilizing the learning progress. ReLU activation functions ensure that non-linearity is introduced into the model so that the network can capture even more complex data relationships.

Max-pooling operations are utilized to achieve downscaling within the encoder. This process effectively reduces the spatial resolution of the feature maps, simultaneously enhancing the network's robustness against minor translational variations in the input. Such downscaling also enlarges the receptive field for the subsequent layers, permitting the network to encapsulate more global and relevant features for segmentation tasks. At the core of the

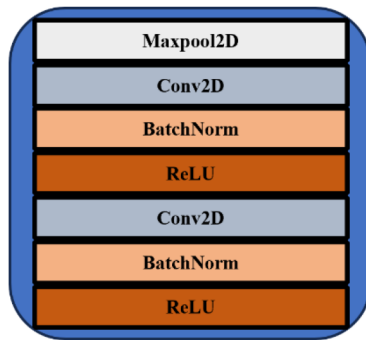


Fig. 1. A single block of DeepSkinSeg encoder.

network resides the bottleneck layer, which occupies a strategic position between the encoder and decoder modules.

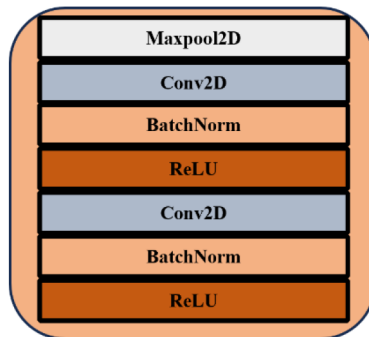


Fig. 2. DeepSkinSeg Bottleneck block.

This layer is characterized by the lowest spatial resolution within the network architecture, compelling the compression of essential information into a highly abstract form. It is in this region that the network distills the most pivotal features needed for accurate segmentation map reconstruction.

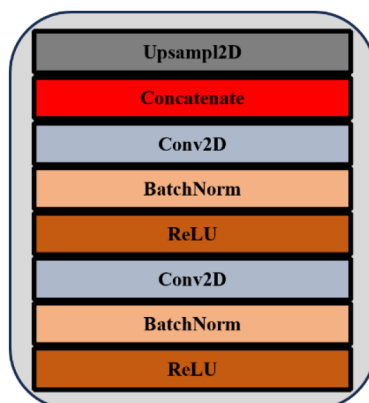


Fig. 3. A single block of DeepSkinSeg decoder.

The decoder, on the other hand, serves as a reflective counterpart to the encoder. The decoder progressively reinstates the feature maps to their original spatial dimensions. It employs up-sampling

layers to escalate the feature map resolution and concatenation operations that synergize these up-scaled features with the corresponding feature maps from the encoder. This integration is facilitated through the application of skip connections, ensuring that both high-level and low-level feature details are harmoniously fused to refine the segmentation outcome.

The method is based on encoding and decoding in the input image, which results in an accurate map of segmentation. With very high accuracy, it segments and gives an output where all the pixels are delimited, making clear the lesion from the surrounding skin tissue. Care is taken for the structure of each block inside the encoder and decoder, performing either feature abstraction or spatial reconstruction so that the network learns and interprets complex patterns required for effective skin lesion segmentation throughout the network. This design methodology focuses on the architecture for DeepSkinSeg and, in a way, its application in medical images, which has great potential and high significance in enhancing segmentation accuracy compared to existing methods. These skip connections are essential in that they allow the recovery of spatial information lost during downscaling so that fine detail for the segmentation of the image is produced in the decoder.

On top of that, DeepSkinSeg adds one more layer: a 1×1 convolutional layer with the objective of mapping the high-dimensional feature maps to the output channels, which have one channel per each class of the segmentation task. A sigmoid activation function is applied to obtain a probability map for the lesion appearance at that pixel. Training of DeepSkinSeg was end-to-end, training and validating with respect to the PH2 dataset and the pairs of images and their corresponding ground truth masks pertaining to the HAM10000 dataset. For the training of DeepSkinSeg, we meticulously chose a set of hyperparameters to optimize the model's performance for skin lesion segmentation tasks. The hyperparameters were selected based on preliminary experiments and literature on best practices for training deep convolutional networks for medical image analysis.

4. Experimental results

We have used the dataset for both training and validation provided in PH2 and HAM10000, as both are considered benchmark databases that contain very high-quality images of dermoscopic lesions in the skin. It provides diversity in the type of skin lesions for the generalization of the model. Moreover, the two datasets were split into training, validation, and testing in order to make a robust model evaluation.

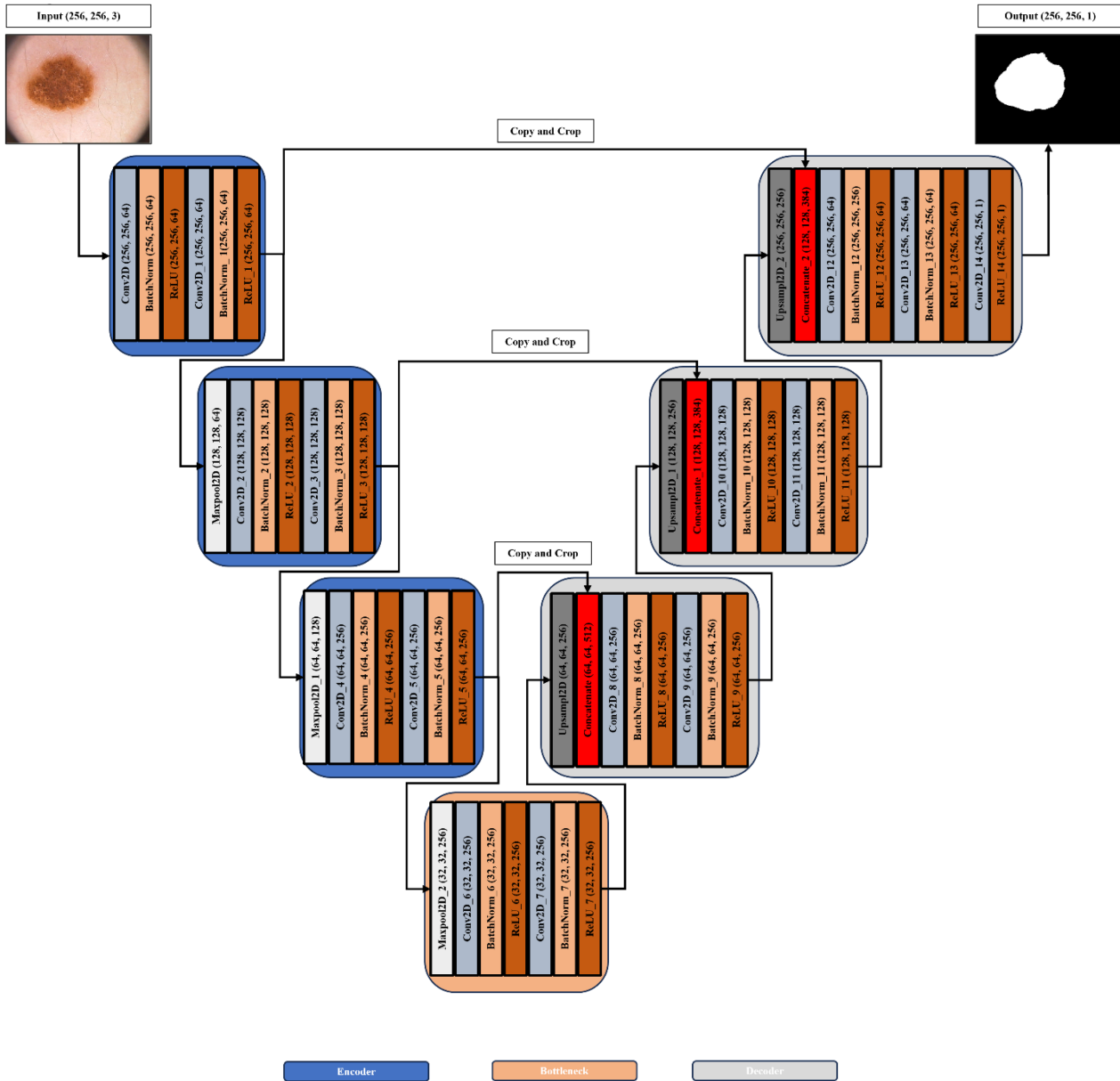


Fig. 4. DeepSkinSeg architecture.

We used an 80-10-10 split ratio, which led to 80% for training data, 10% for validation data, and the same for testing.

4.1. Data pre-processing

We apply different pre-processing techniques to data that can help improve the performance and robustness of the model. First, all the images were resized in such a way that they had a uniform resolution of 256×256 pixels. Then, the pixel values of the images and masks were normalized to the $[0, 1]$ range for stability during training.

4.2. Loss function, optimizer, and evaluation metrics

For segmentation as a binary task, the network was trained with binary cross-entropy as a loss function and Adam as an optimizer with a learning rate of $1e-5$. During the training and evaluation, the following focus was given over the key metrics that would be used in order to present the work performance of DeepSkinSeg.

$$IoU = \frac{2 \times TP}{2 \times TP + FP + FN} \quad (1)$$

$$Dice = \frac{TP}{TP + FP + FN} \quad (2)$$

$$Precision = \frac{TP}{TP + FP} \quad (3)$$

$$Sensitivity = Recall = \frac{TP}{TP + FN} \quad (4)$$

$$Accuracy = \frac{(TP + TN)}{(TP + TN + FP + FN)} \quad (5)$$

$$Specificity = \frac{TN}{TN + FP} \quad (6)$$

$$F1\ Score = 2 \times \frac{Precision \times Sensitivity}{Precision + Sensitivity} \quad (7)$$

With these metrics, we aimed to comprehensively evaluate DeepSkinSeg's performance in capturing lesion boundaries and accurately segmenting skin lesions.

5. Hyperparameters and results

Table 1 provides an overview of the hyperparameters used in DeepSkinSeg. However, following 50 training epochs, the DeepSkinSeg model gave a mean loss of 0.2496. Remarkably, the IoU score amounted to 0.9170, which revealed a high overlap between the predicted and ground truth lesion masks. A dice coefficient of 0.9564 further shows the ability of the model to conduct accurate skin lesion segmentation. The values of these two parameters are in the range of 0.9789 for specificity and 0.9792 for sensitivity, which shows their ability to identify skin lesion regions precisely. Additionally, the model exhibited an outstanding accuracy of 0.9857 during the training phase.

Table 1. Summarizing the hyperparameters of DeepSkinSeg.

Hyperparameter	Value
Batch Size	10
Number of Epochs	50
Learning Rate	0.00001
Optimizer	Adam
Loss function	Cross-Entropy
Total params	4,842,497
Trainable params	4,837,889
Non-trainable params	4,608

On the other hand, validation performance was thoroughly tested, and all those images were never seen during training. In this part, the DeepSkinSeg architecture achieved a mean loss of 0.3596 and, therefore, had good generalization power. More importantly, the model was able to secure an IoU score of 0.7672, signifying that there is quite an overlap between the predicted masks and the ground truth. The high value of the Dice coefficient, estimated at 0.8682, ascertains that the model is accurate in the delineation of skin lesions. Besides, the model upheld a recall value of 0.9312, which is acceptable, thus showing that the identified skin lesion regions are reliable. However, the value of the recall for this phase was observed at 0.8548, an indication of reduced sensitivity from the training phase. The model, however, showed excellent accuracy at 0.9481, meaning it can classify pixels well in skin lesion segmentation. These results point out the efficacy of DeepSkinSeg architecture in the precise segmentation of skin lesions, which is significant for medical diagnosis and treatment planning. It performs with a competitive spirit, i.e., for training and generalization, and highly recommends its candidacy as a resourceful utility in dermatological applications.

The model's high IoU and Dice Coefficient values during both training and validation times have solidified consistent and accurate skin lesion segmentation. Very high values for precision and recall illustrate the remarkable ability of the model to identify boundaries and regions of the skin lesion faithfully. The very high accuracy scores show the effectiveness of the model in classifying skin lesion pixels. These findings certify the adequacy of the proposed DeepSkinSeg architecture in providing a light but powerful solution for the accomplishment of skin lesion segmentation tasks. These findings place DeepSkinSeg as an up-and-coming field within the world of dermatology, which could optimize the process of skin lesion analysis and be useful for healthcare personnel to make clinical decisions accurately and promptly. We present the performance evaluation of DeepSkinSeg on the PH2 dataset in Table 1. In addition, Figs. 1 to 3 illustrate insights into the performance of the network based on loss with accuracy, recall with precision, and IoU with Dice Coefficient metrics.

Fig. 5 illustrates the loss curves and accuracy for training and validation over 50 epochs for both PH2 and HAM10000 datasets, respectively. The training loss is monotonically decreased, which means that the network learns to minimize segmentation errors. Also, from the validation loss curve, one can see that it is decreasing, which means that DeepSkinSeg generalizes well with unseen data. Similarly, from the

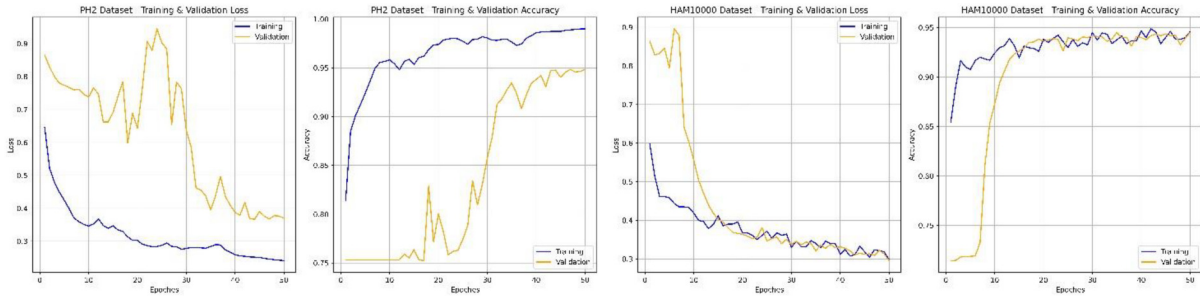


Fig. 5. Training and validation loss and accuracy for PH2 (left) and HAM10000 (right) datasets.

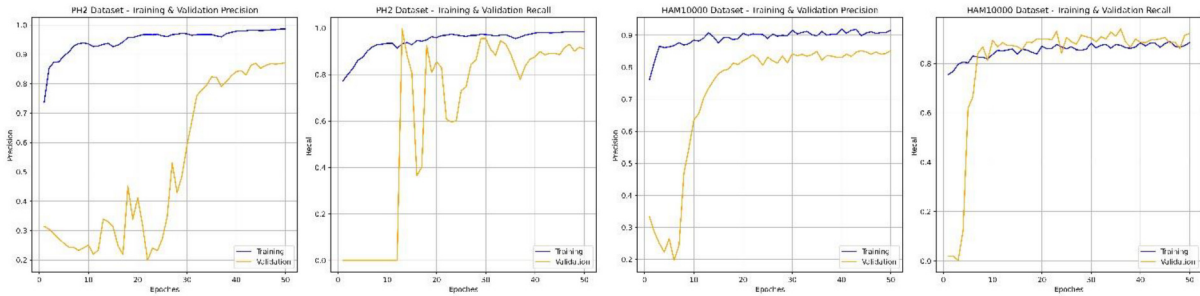


Fig. 6. Training and validation recall and precision for PH2 (left) and HAM10000 (right) datasets.

training and validation accuracy curves, the network can give an accurate prediction of the boundary of the lesion.

Fig. 6 depicts the trend of the network’s performance in terms of recall and precision for both PH2 and HAM10000 datasets, respectively. High recall indicates the capture of a more significant number of true-positive cases by DeepSkinSeg, whereas precision indicates the network’s ability to keep the number of false positives low. The ideal trade-off between recall and precision is needed to get perfect skin lesion area segmentation.

Fig. 7 presents the IoU and Dice Coefficient metrics for both PH2 and HAM10000 datasets, respectively, which define the most common metrics of the segmentation accuracy of the models. IoU and Dice’s coefficients are statistical techniques employed to

measure the level of similarity between the predicted image masks and the ground truth image masks. Both large IoU and large Dice values imply high agreements between the predicted masks and actual masks, showing that the network outlines the skin lesions well.

Fig. 8 presents the performance evaluation of our DeepSkinSeg model regarding the PH2 and HAM10000 datasets, respectively. Furthermore, Table 2 illustrates the rapid progression and enhancement in the domain of skin lesion segmentation models. Among the key takeaways is the consistent improvement across various metrics such as accuracy, sensitivity, and the Dice coefficient, showcasing the advancements in computational methods and the increasing sophistication of deep learning algorithms applied in dermatological research.

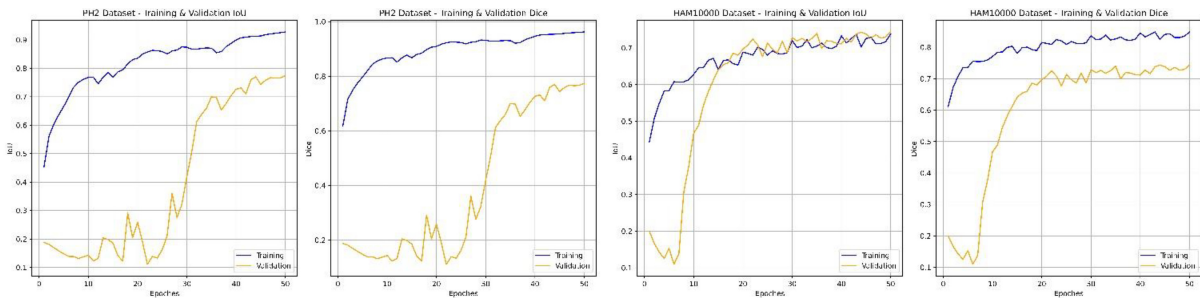


Fig. 7. Training and validation recall and precision for PH2 (left) and HAM10000 (right) datasets.

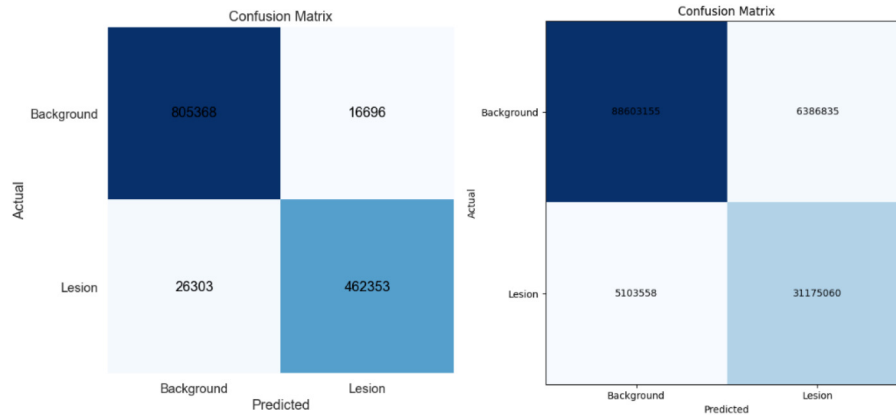


Fig. 8. Confusion matrix for the testing set regarding the PH2 (left) and HAM10000 (right) datasets.

Table 2. Different methods performance regarding the Ph2 dataset.

Authors	Year	Accuracy	Sensitivity	Precision	Dice	IoU	Specificity	F1-Score
Tang et al. [13]	2019	96.69	96.51	N/A	94.13	89.40	95.26	N/A
Qiu et al. [14]	2020	95.58	N/A	N/A	93.48	88.50	N/A	N/A
Tang et al. [15]	2020	95.71	N/A	N/A	93.36	88.21	N/A	N/A
Dayananda et al. [16]	2021	97.00	N/A	N/A	94.00	89.00	N/A	N/A
Hu et al. [17]	2022	95.20	96.24	N/A	93.05	87.60	94.31	N/A
Deepa and Madhavan [18]	2023	96.29	96.27	96.30	94.53	89.63	N/A	N/A
Dong et al. [19]	2024	N/A	94.11	95.97	N/A	90.53	N/A	95.03
Li et al. [20]	2024	92.40	93.60	N/A	88.90	80.10	93.10	N/A
Srikanteswara and Ramachandra [21]	2024	96.95	N/A	N/A	93.98	89.14	N/A	N/A
DeepSkinSeg	2024	96.72	96.84	97.97	95.56	91.49	96.51	97.40

DeepSkinSeg marks a pinnacle in this evolving landscape, demonstrating exceptional performance across nearly all evaluated metrics. The notable achievements in precision (97.97%), Dice coefficient (95.56%), and IoU (91.49%) underscore DeepSkinSeg’s ability to precisely delineate lesion boundaries, which is critical for accurate diagnosis and treatment planning.

Table 2 also highlights the varied focus and reporting standards among different studies, with some prioritizing metrics like specificity and others emphasizing the balance between recall and precision, as evidenced by F1 scores. The presence of Not Available “N/A” entries suggests a selective emphasis or possible challenges in measuring specific metrics, indicating an area for future standardization in reporting. Moreover, DeepSkinSeg’s superiority in balancing sensitivity and precision, along with its high F1 score, points to its robustness and reliability, making it a potentially invaluable tool for clinicians.

Table 3 displays the performance of the different segmentation methods applied to the HAM10000 benchmark dataset in dermatology for skin lesion analysis. DeepSkinSeg model presents several advantages in skin lesion segmentation. First, it prudently discards the number of layers to ensure that the segmentation is powerful and keeps the model rel-

atively light in computation. While, more often, such characteristics are missed by more complex and up-to-date architectures, this allows for catering to the ever-increasing demand for real-time and resource-conscious applications in the field of medical imaging.

DeepSkinSeg is oriented to the fine details in the lesion. It allows for a better diagnosis and medical planning. We fully validate DeepSkinSeg in the datasets PH2 and HAM10000 to guarantee consistency with the benchmark of skin lesion analysis. Again, this result was consistent with high IoU, Dice Coeff., and accuracy, confirming the superiority and efficacy of the DeepSkinSeg model for accurate lesion contouring.

Our DeepSkinSeg scores entirely high in metrics, with accuracy at 94.60%, precision at 97.65%, sensitivity at 95.11%, F1 at 96.36, highest Dice at 96.36, Jaccard at 92.98% coefficients, and specificity at 93.04%. Our proposed DeepSkinSeg model demonstrates balanced and superior performance in identifying both the lesion and non-lesion area rightly with high precision and efficiency. The boundaries by DeepSkinSeg are more aligned with the ground truth, both in terms of smoothness and accuracy. Especially for more complex and irregular lesions, DeepSkinSeg outperforms UNet.

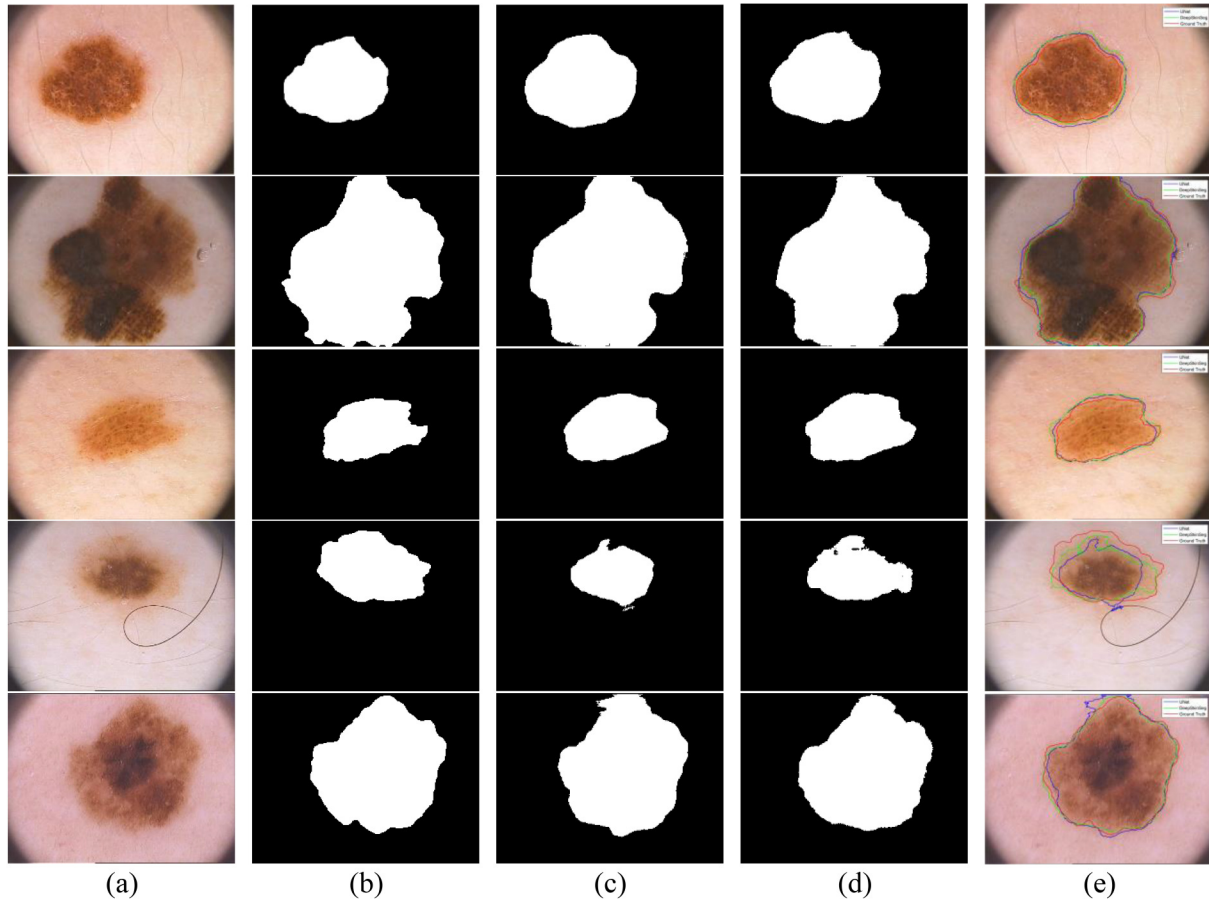


Fig. 9. Segmentation comparison for the PH2 test set: (a) Original image, (b) Ground truth, (c) UNet, (d) DeepSkinSeg, and (e) Boundary.

Table 3. Different methods performance regarding the Ham10000 dataset.

Authors	Year	Accuracy	Sensitivity	Precision	Dice	IoU	Specificity	F1-Score
Basak et al. [22]	2022	N/A	99.99	N/A	90.60	90.20	99.99	90.30
Tomar et al. [23]	2022	92.35	86.50	96.11	N/A	80.23	N/A	87.31
Namburu et al. [24]	2023	90.50	95.20	N/A	83.00	85.60	86.20	N/A
Yang et al. [25]	2023	96.46	N/A	N/A	93.59	88.81	N/A	N/A
Zhang et al. [26]	2024	N/A	N/A	N/A	83.10	74.33	N/A	N/A
DeepSkinSeg	2024	94.60	95.11	97.65	96.36	92.98	93.04	96.36

It is clear from Fig. 11 that both models demonstrate reasonable segmentation performance, but DeepSkinSeg frequently delivers results that more closely align with the ground truth. Additionally, DeepSkinSeg tends to produce smoother and more accurate boundaries compared to UNet, especially for more oversized and irregular lesions. In contrast, UNet's boundaries occasionally over-segment or under-segment the lesion, resulting in discrepancies.

6. Conclusions

In this paper, we propose a new architecture based on UNet to solve the task of skin lesion segmentation. The main contribution of this work is the develop-

ment of a lightweight network that can still retain the efficacy of UNet but with a fewer number of layers, making the model computationally more efficient and not adversely affecting the segmentation accuracy. DeepSkinSeg provides a dedicated solution to the problem of skin lesion segmentation. We have adopted a model that focuses attention on acquiring fine details of the lesion and delineates the boundary of the lesion very accurately by optimizing the architecture of UNet. This network reconciles the accuracy of computation and segmentation, and therefore, it becomes a good tool for dermatological analysis. We evaluate the efficiency of DeepSkinSeg, using the widely known PH2 dataset as benchmark data in skin lesion studies. The results were quite effective in showing that our network was able to produce

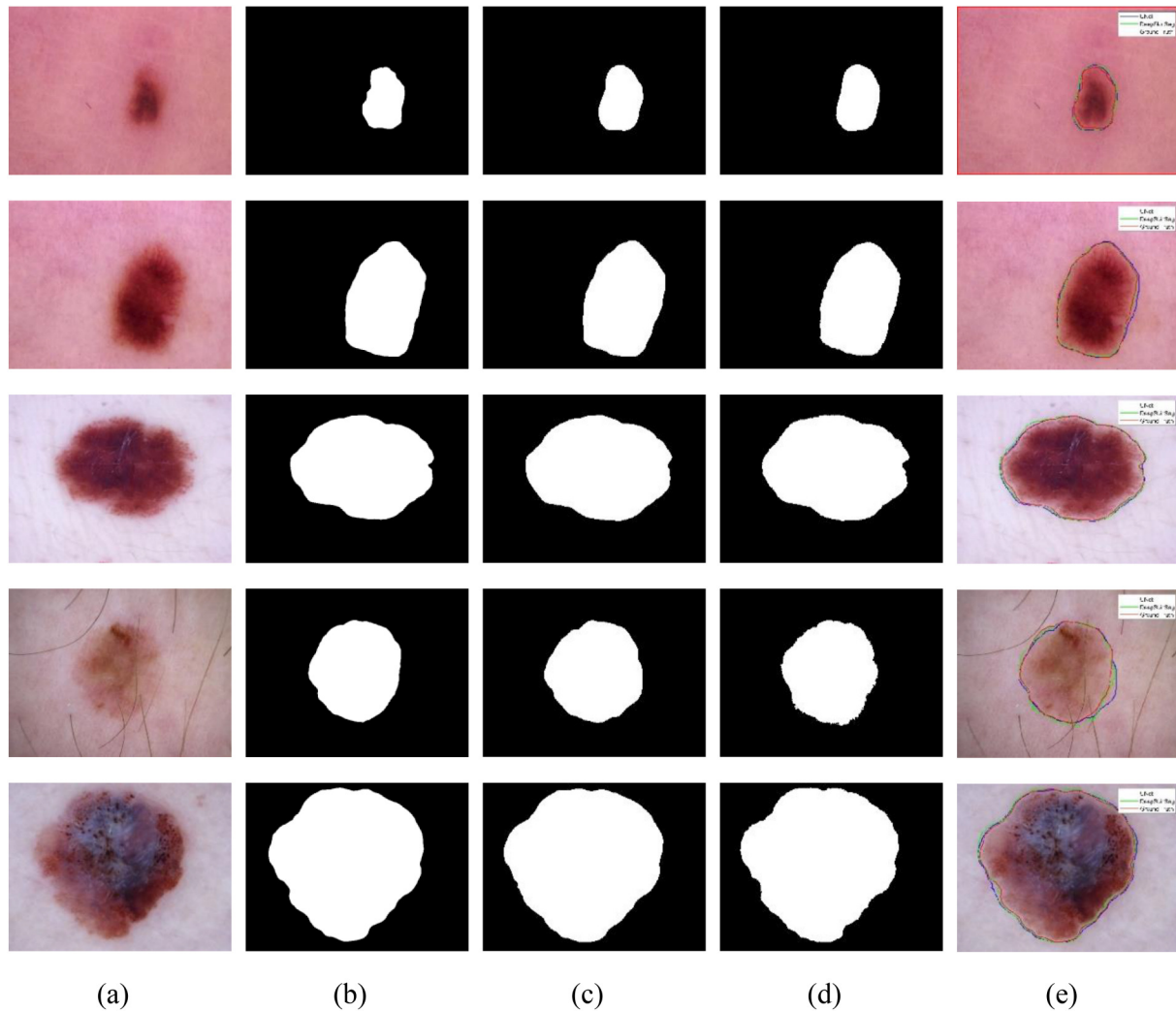


Fig. 10. Segmentation comparison for the HAM10000 test set: (a) Original image, (b) Ground truth, (c) UNet, (d) DeepSkinSeg, and (e) Boundary.

high IoU, good Dice coefficient, and high accuracy, which brings out the capability of our network in segmenting skin lesions accurately. This is clinically of immense value for the early diagnosis of the disease entity and the planning of treatment, as many require intricate details and some superficially subtle. During our evaluation, we report the visual segmentation results of 20 test images drawn from the PH2 dataset and 1001 test images from the HAM10000 dataset, along with the performance metrics on a large scale. In the overall analysis, DeepSkinSeg exhibited the utmost precision and reliability in skin lesion segmentation, which further puts an emphasis on its potential to be put into clinical use.

Conflicts of interest

The authors declare no conflict of interest.

Author contributions

Fallah H. Najjar: conceptualization, data creation, formal analysis, and writing the original draft. Prof. Dr. Farhan Mohamed and Prof. Dr. Mohd Shafray supervised the writing and editing of the final draft. Asniyani Nur Haidar: formal data analysis and resources. Karrar A. Kadhim: conceptualization and writing the original draft.

References

1. D. G. Chawla *et al.*, “Benchmarking transcriptional host response signatures for infection diagnosis,” *Cell Systems*, vol. 13, no. 12, pp. 974–988, e7, 2022.
2. L. Parizotto *et al.*, “Modern medicine relies on the help of microorganisms—from vaccine production to cancer medication,” *Good Microbes in Medicine, Food Production, Biotechnology, Bioremediation, and Agriculture*, pp. 1–12, 2022.

3. D. Petrova *et al.*, “The patient, diagnostic, and treatment intervals in adult patients with cancer from high-and lower-income countries: A systematic review and meta-analysis,” *PLoS Medicine*, vol. 19, no. 10, p. e1004110, 2022.
4. D. Crosby *et al.*, “Early detection of cancer,” *Science*, vol. 375, no. 6586, p. eaay9040, 2022.
5. S. Foser *et al.*, “Looking to the future of early detection in cancer: Liquid biopsies, imaging, and artificial intelligence,” *Clinical Chemistry*, vol. 70, no. 1, pp. 27–32, 2024.
6. M. Ciałżyńska *et al.*, “The incidence and clinical analysis of non-melanoma skin cancer,” *Scientific reports*, vol. 11, no. 1, p. 4337, 2021.
7. J. Malvey and G. Pellacani, “Dermoscopy, confocal microscopy and other non-invasive tools for the diagnosis of non-melanoma skin cancers and other skin conditions,” *Acta Dermato-Venereologica*, vol. 97, pp. 22–30, 2017.
8. T. Saba, “Computer vision for microscopic skin cancer diagnosis using handcrafted and non-handcrafted features,” *Microscopy Research and Technique*, vol. 84, no. 6, pp. 1272–1283, 2021.
9. H. Li *et al.*, “An improved deep learning approach for detection of thyroid papillary cancer in ultrasound images,” *Scientific reports*, vol. 8, no. 1, p. 6600, 2018.
10. S. Inthiyaz *et al.*, “Skin disease detection using deep learning,” *Advances in Engineering Software*, vol. 175, p. 103361, 2023.
11. T. Ugai *et al.*, “Is early-onset cancer an emerging global epidemic? Current evidence and future implications,” *Nature Reviews Clinical Oncology*, vol. 19, no. 10, pp. 656–673, 2022.
12. S. R. Waheed *et al.*, “Melanoma skin cancer classification based on CNN deep learning algorithms,” *Malaysian Journal of Fundamental and Applied Sciences*, vol. 19, no. 3, pp. 299–305, 2023.
13. P. Tang *et al.*, “Efficient skin lesion segmentation using separable-Unet with stochastic weight averaging,” *Computer Methods and Programs in Biomedicine*, vol. 178, pp. 289–301, 2019.
14. Y. Qiu *et al.*, “Inferring skin lesion segmentation with fully connected CRFs based on multiple deep convolutional neural networks,” *IEEE Access*, vol. 8, pp. 144246–144258, 2020.
15. Y. Tang *et al.*, “Imscgnet: Iterative multi-scale context-guided segmentation of skin lesion in dermoscopic images,” *IEEE Access*, vol. 8, pp. 39700–39712, 2020.
16. C. Dayananda *et al.*, “Skin lesion segmentation in dermoscopic images using CNN architecture,” in *2021 International Conference on Information and Communication Technology Convergence (ICTC)*, IEEE, 2021.
17. K. Hu *et al.*, “AS-Net: Attention synergy network for skin lesion segmentation,” *Expert Systems with Applications*, vol. 201, p. 117112, 2022.
18. J. Deepa and P. Madhavan, “ABT-GAMNet: A novel adaptive boundary-aware transformer with gated attention mechanism for automated skin lesion segmentation,” *Biomedical Signal Processing and Control*, vol. 84, p. 104971, 2023.
19. Z. Dong, J. Li, and Z. Hua, “Transformer-based multi-attention hybrid networks for skin lesion segmentation,” *Expert Systems with Applications*, vol. 244, p. 123016, 2024.
20. X. Li *et al.*, “USL-Net: Uncertainty self-learning network for unsupervised skin lesion segmentation,” *Biomedical Signal Processing and Control*, vol. 89, p. 105769, 2024.
21. R. Srikanteswara and A. Ramachandra, “ACM technique for recognition of region of interest using contour and colour features,” *Multimedia Tools and Applications*, pp. 1–13, 2024.
22. H. Basak, R. Kundu, and R. Sarkar, “MFSNet: A multi focus segmentation network for skin lesion segmentation,” *Pattern Recognition*, vol. 128, p. 108673, 2022.
23. N. K. Tomar *et al.*, “Fanet: A feedback attention network for improved biomedical image segmentation,” *IEEE Transactions on Neural Networks and Learning Systems*, 2022.
24. A. Namburu *et al.*, “Skin cancer segmentation based on triangular intuitionistic fuzzy sets,” *SN Computer Science*, vol. 4, no. 3, p. 228, 2023.
25. L. Yang *et al.*, “Rema-Net: An efficient multi-attention convolutional neural network for rapid skin lesion segmentation,” *Computers in Biology and Medicine*, vol. 159, p. 106952, 2023.
26. Z. Li *et al.*, “SG-MIAN: Self-guided multiple information aggregation network for image-level weakly supervised skin lesion segmentation,” *Computers in Biology and Medicine*, vol. 170, p. 107988, 2024.